Desalination and Water Treatment
www.deswater.com

doi: 10.5004/dwt.2017.0061

58 (2017) 12–18
January

Empirical parameterization of solar still performance

Aasim A. Azooz*, Ghada G. Younis

Department of Physics, College of Science, Mosul University, Mosul, Iraq, Tel. +9647703035073; email: aasimazooz1@yahoo.com (A.A. Azooz); Tel. +964 7704120345; email: ghada.ghanim@yahoo.com (G.G. Younis)

Received 15 January 2016; Accepted 1 June 2016

ABSTRACT

Experimental data on the operation of a simple inclined surface solar still are analyzed for the purpose of obtaining an empirical equation relating the amount of fresh water collected to the total amount of solar energy per day (S), the maximum atmospheric temperature (T), and the mean wind speed (W). The solar still used has a 1 m^2 effective area with a 25° inclined glass cover. The empirical model is based on the assumption that the solar, temperatures, and wind, have combined linear effects on the still efficiency. Good agreement between experimental data and model predictions is obtained for both our data and some independent literature published experimental data. Results also indicate that the amount of the total daily solar energy represents the dominating factor governing the still daily productivity compared with temperature and wind effects.

Keywords: Solar still; Desalination; Solar desalination; Single inclination

1. Introduction

Life on the planet earth is water-based one. Human life and civilizations have always centered on locations with available fresh water resources. However, increased world population has put the future of fresh water availability at a challenge [1–4]. Global warming caused to enhance the problem of the world water shortage [5,6]. Armed conflicts caused by competition over water are expected to increase during the twenty-first century [7,8] unless the world water shortage problem is fully addressed.

In order to utilize the abundantly available seawater, many countries have resorted to seawater desalination to supply parts of their needs. Two major types of desalination methods are widely used. These are the phase change method and the reverse osmosis method [9]. Although the latter method is more energy efficient, it does involve higher capital investment. Even so, it is a well-known fact that both methods involve high power consumption [10]. This issue is gaining more significance due to the increased concerns about climate change associated with increasing carbon dioxide emissions [11,12].

More considerations are now being paid toward using renewable energies for seawater desalination [13,14]. The two most attractive candidates for such processes are wind and solar power. Solar desalination in particular has been in use although on some limited scale for many years [15]. The traditional solar still in its many shapes, designs, and geometrical configurations is considered the most popular method [16]. This is due to its design and construction simplicities, and its low construction, operation, and maintenance costs.

In spite of its simplicity, the solar still operation theory is rather complicated compared with phase change and reverse osmosis methods. This is because of the many interacting thermodynamical processes involved in the evaporation, heat exchanges, and condensation processes. This has resulted in using approximations, simulations, and numerical calculations methods [17–29] rather than exact analytical methods to predict the still operation. This makes a good case for attempting to construct some empirical model based on experimental results to predict the performance of any solar still under various real life environmental conditions. The present work is concerned with such attempt.

* Corresponding author.

1944-3994/1944-3986 © 2017 Desalination Publications. All rights reserved.

2. Experimental setup

The solar still used in this work is a simple homemade one. It is a 1 m^2 (125 cm × 80 cm × 10 cm) rectangular basin constructed from folded angles aluminum sheet plate. The sketch diagram of the still is shown in Fig. 1(a). The bottom of the basin is black painted. The basin is covered with 6 mm thick ordinary glass inclined at 25° to the horizontal. The still is thermally insulated from the bottom and all sides using ordinary 2.5 cm thick plastic foam. The water depth is kept constant at about 5 cm using a floating water feed valve. The picture of the completed solar still used is shown in Fig. 1(b). The water condensed on the glass surface is collected via a horizontal channel into 5-l plastic container.

The minuet-by-minuet solar irradiation and total daily solar energy data were measured at home using cosine corrected solar radiation meter PCE-SPM 1 supplied by Tursdale Technical Services Ltd., UK [30]. The instrument has a computer logging system.

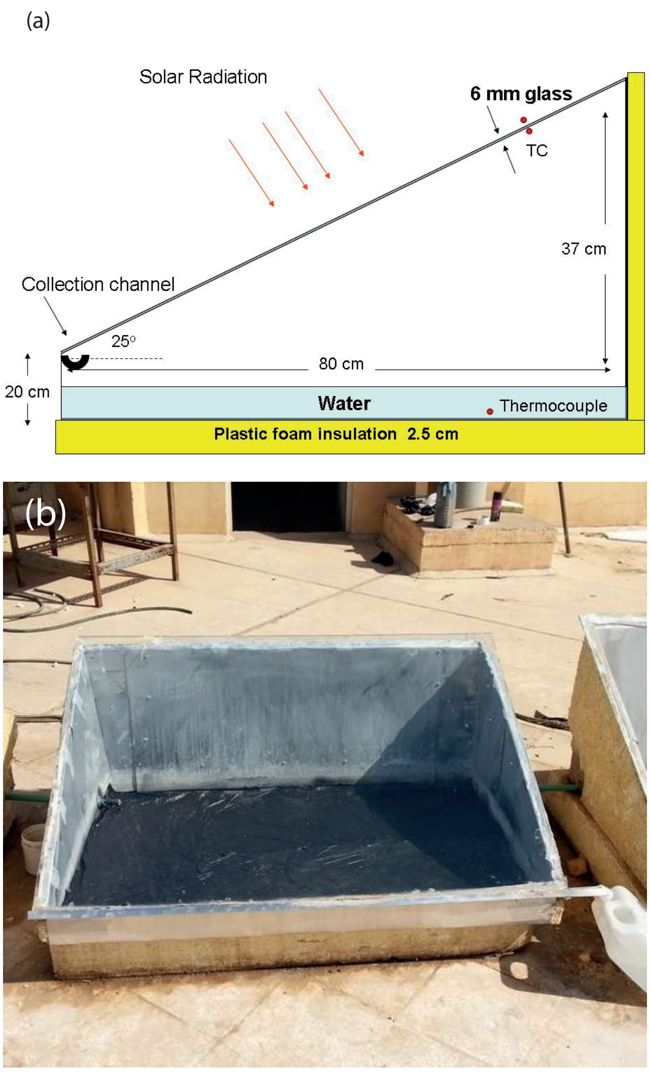

Fig. 1. Experimental solar still: (a) sketch diagram (lateral view) and (b) actual basin.

3. Experimental procedure

It may be worth pointing out that this work was carried out at physics department – Mosul University. Mosul city in Iraq is situated at 36.3400° N, 43.1300° E. Mosul climate is considered as Semiarid-Cold-Desert (BWk) according to the Köppen-Geiger climate classification [31]. Temperatures can vary between –10°C in winter and 52°C on July summer days. Wind speed is in the range of 0–50 km h^{-1}. This wide range of climate variations covers almost all types of conditions where solar desalination can be fruitfully used. The distributions of maximum, mean, and minimum temperatures and wind speeds covering one-year period are presented in Figs. 2 and 3, respectively. The two figures demonstrate the wide variations in Mosul weather conditions.

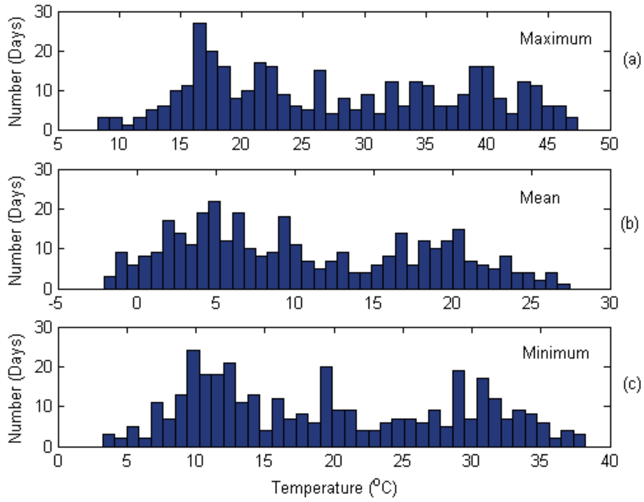

Fig. 2. (a) Maximum, (b) mean, and (c) minimum daily temperatures distribution in Mosul for between first of November 2014 and end of September 2015.

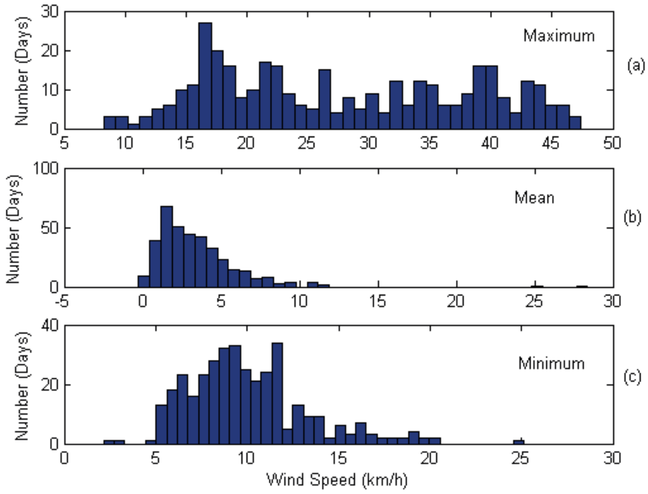

Fig. 3. (a) Maximum, (b) mean, and (c) minimum daily wind speed distribution in Mosul for between first of November 2014 and end of September 2015.

Table 1
Accuracies, ranges and standard uncertainties of all instruments and methods used in this work

	Instrument	Accuracy	Range	Standard uncertainty
1	Solar radiation meter PCE-SPM 1	1 w m^{-2}	0–2,000 w m^{-2}	0.38 w m^{-2}
2	Chunshop WH5001 digital thermometer temperature meter gauge C/F	0.1°C	–50°C–110°C	0.05°C
3	Digital weight meter	1 gm	0–5,000 gm	0.5 gm
4	Ambient temperature Measurement [32,33]	1°C	–10–60	2%
5	Wind speed measurement [32,33]	0.5 m s^{-1}	0–100 m s^{-1}	2%

The original plan for data collection was to acquire daily water production from the still over a complete one-year period. This would have covered almost the widest range of weather conditions. However, and at just before the start of the planned data collection in June 2014, the city fell under armed group, and access to the site became impossible until November 2014. Even by then, it was not possible to access the site on daily basis. Even so, over the period from November 2014 to end of July 2015, arrangements for collecting 80 daily-condensed water data could be made. By the end of July 2015, it became impossible to continue the work. The data collected cover a reasonably wide range of weather variations, as autumn months in Mosul are almost similar to those for spring.

A more serious problem was related to obtaining creditable daily Mosul weather data for the period under consideration. Mosul weather station, which was planned to be the source of such data, has seized operation. An alternative weather data source was found. The weather data for the days involved were obtained from meteoblue weather site [32]. This site provides reasonably accurate access to past weather simulations for every place in the world. However, these data are published in graphical form and a special matlab image processing software is used to extract numerical data from the graphs presentations. The software structure and operation is described in reference [33]. This software is capable of converting digital images of graph plot or signals on oscilloscope screens to numerical values. The software is used to obtain numerical values of maximum, minimum, and mean temperatures, together with wind speed for all dates of the experiment. The extracted numerical data are accurate within 2% error. The accuracy of the combined simulated graphical data and the image processing technique used were cross-checked through comparing them with actual historical data acquired by Mosul weather station for dates before its shutdown. All data are used to build a database for further analysis purpose.

The accuracies, ranges, and standard uncertainties of all instruments and methods used are summarized in Table 1.

Fig. 4 shows the amount of water collected for each of the days involved in the experiment. Day 1 is November 24, 2014. The amount of water collected per day is corrected for possible loss by evaporation. This loss is obtained by measuring the amount of water lost from a similar container filled with 1 l of water placed beside the solar still. The average loss amounted to only few cm^3 per day.

4. Modeling, results and discussion

There are many experimental published works on building and studying the performance of different types and

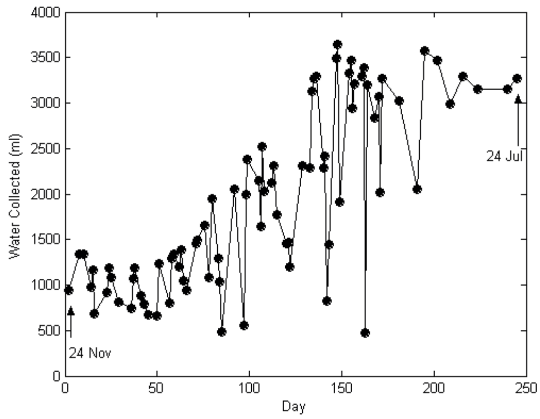

Fig. 4. The amount of distilled water produced by the still over the entire experiment.

configurations of solar stills in different parts of the world. The aims of most of these studies are concerned with construction materials, glass optical and thermal properties, geometrical designs, assisted evaporation, convection and condensation procedures involved, and their effects on the still productivity [34–48]. The purpose of this experiment is to acquire sufficient amount of experimental data for the still operation under the widest possible range of weather conditions. These data are used in building an empirical model relating the still desalinated daily water productivity to varying weather conditions

The first step in such modeling is to specify the main weather factors affecting the still operation. These factors are:

(1) the total solar radiation over the entire daylight period (S);
(2) the maximum temperature during daylight time (T); and
(3) the mean wind speed (W).

All other weather parameters including cloud cover, relative humidity, water temperature and so on are implicitly included within the above three main parameters. It may be worth mentioning here that the maximum daytime temperature rather than the mean temperature is considered here as the effective parameter. This is because most evaporation takes place during the day and mean temperatures are usually calculated using minimum night temperatures. It can thus be argued that the amount of distilled water (M), produced per day by the still can be written as the linear combination of three functions $F(S)$, $G(T)$, and $H(W)$. Thus, we may write as follows:

$$M(S,T,W) = a_1F(S) + a_2G(T) + a_3H(W) \tag{1}$$

where a_1, a_2, and a_3 represent the fractional contribution of each of the corresponding three effects.

However, and before one proceeds in applying the above modeling, some investigation of the true independency between the three variables is worth discussing. For this purpose, the data for the entire one-year relating wind speed to maximum temperature are plotted in Fig. 5. It is clear from the figure that there is no correlation between these two variables. The application linear correlation regression to the data produced a correlation coefficient of 0.0069 with 95% confidence level coefficient range of –0.0269–0.0506 resulting in the acceptance of the null hypothesis. It can thus be safely assumed that these two variables are highly independent of each other.

The correlation between the total daily solar power and mean wind speed is shown in Fig. 6. No convergent with 95% confidence level linear correlation fit could be found. The main conclusion here is that these two variables are completely independent.

As far as the independency of total solar radiation (S) and maximum temperature (T) is concerned, it is trivial to say that these two variables are strongly correlated. However, and from purely phenomenological point of view, these two variables can be treated as independent of each other. This is mainly because of their different roles in the solar still operation. This can be explained by the fact that while the main effect of increased solar radiation is related to increasing temperatures of water, glass, and atmosphere causing increased evaporation, the effect of atmospheric temperature is the cooling of the glass, which assists condensation process. The two phenomena are independent of each other. This is demonstrated in Figs. 7 and 8. Fig. 7 suggests an approximately linear relationship of M to S, while the relation of M to T in Fig. 8 is more complicated. This will be discussed later.

If we consider that each of the above three functions F, G, and H to be a monotonic function of its corresponding independent variable, and refer the observed fluctuations in experimental data as signatures of the other two variables, the task reduces to finding each one of three functions independently. To achieve such purpose, the amount of daily-distilled water produced is plotted against each of the three parameters in Figs. 7, 8, and 9 independently. The data on each plot are sorted in ascending order of the value of the corresponding independent variable. A suitable shape describing mathematical form with free fitting parameters, which best describe the shape of the data in each figure, was

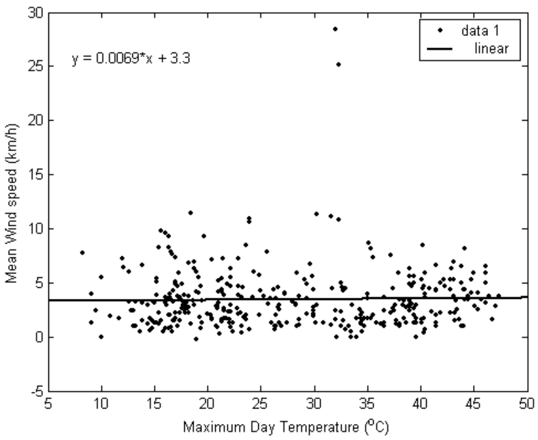

Fig. 5. Correlation between maximum daily temperature and wind speed.

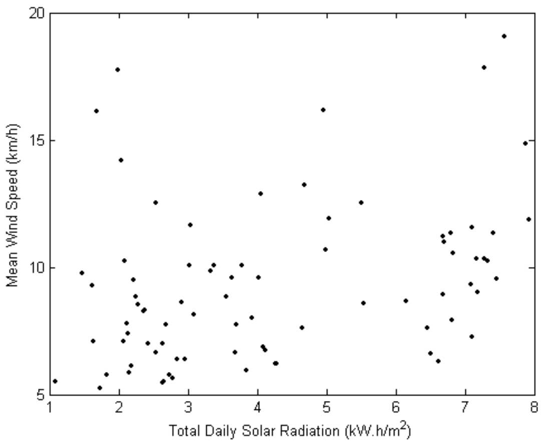

Fig. 6. Correlation between total daily solar power and mean wind speed.

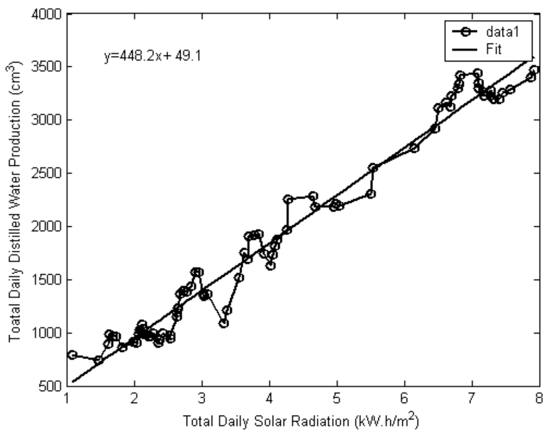

Fig. 7. The amount of water collected plotted vs. total solar radiation for daylight time.

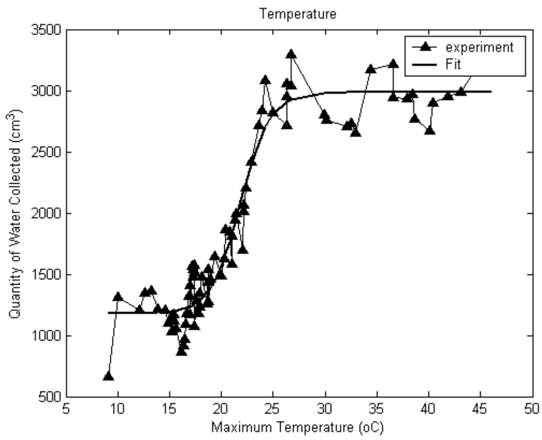

Fig. 8. The amount of collected water plotted against maximum daylight temperature.

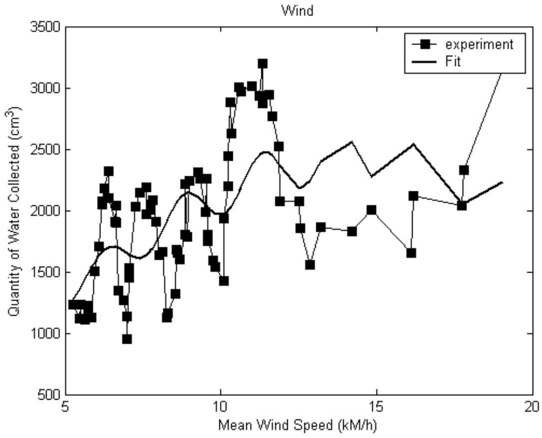

Fig. 9. The amount of water collected plotted against wind speed.

selected. The values of the fitting parameters are left to be determined by the fitting program.

It is reasonably clear from Fig. 7 that the data can be fitted to a linear equation. The 95% confidence level linear equation obtained is as follows:

$$F(S) = 448.2S + 49.1 \tag{2}$$

It is interesting to note that even at zero radiation, this fitted equation gives a value of about 49.1 cm^3 of water. This is consistent with the fact that there is always some evaporation and condensation due to differences in partial pressures.

The situation regarding Fig. 8 is very much different. Although there is a fast dependence of water collected against maximum temperature between 15°C and 25°C, this dependence seems to saturate below and above this range. This confirms the justification for treating T as independent variable from S in our modeling. The two saturation effects clearly demonstrate that there are two regions in temperature, where the still operation becomes almost insensitive to temperature changes. The first region is at temperatures below 15°C. From physical point of view, this is associated with only little evaporation. The second region is at temperatures above 25°C. In this region, and although there is increased evaporation from the still basin, the glass temperature becomes high to a point, which allows for more re-evaporation of condensed water to take place. One good mathematical description of such saturation effect is the tangent hyperbolic type function. Nonlinear fitting of the data to such function gives the following:

$$G(T) = 903.5\tanh\left[\frac{(T-21.8)}{2.86}\right] + 2.3 \tag{3}$$

The situation related to wind speed in Fig. 9 seems more complicated. It was not easy to find a suitable mathematical fitting equation that can best describe the experimental data. However, the following six free parameters fitting equation, which is Gaussian shaped modulated by a sinusoidal equation proved to give the best fit for the experimental data.

$$H(W) = \left[198.4\cos(2.5W - 9.4) + 2427\right] \times \exp\left[\frac{-(W-14.3)^2}{144}\right] \tag{4}$$

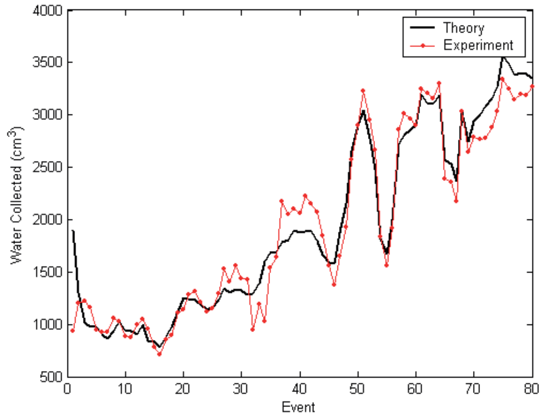

Fig. 10. Red data points represent the quantity of water collected during each particular day of the experiment with particular weather conditions (event). The black sold line represents results of substituting the weather conditions for the particular day into Eq. (1).

Table 2
Model fitting parameters and 95% confidence level ranges

Parameter in Eq. (1)	Best fitted value	95% confidence level range
a_1	0.9973	$0.85 < a_1 < 10.85$
a_2	0.0032	$0.0 < a_2 < 0.17$
a_3	0.0031	$0.0 < a_3 < 0.13$

Substituting for F, G, and H from Eqs. (2)–(4) will give the estimations for water collected per day under any weather conditions. However, the three free parameters a_1, a_2, and a_3, which represent the relative weight of each of the three effects considered, remain to be found. In order to find these parameters, all the data are fitted to Eq. (1) after substitution for F, G, and H with a_1, a_2, and a_3 to be determined by the matlab fitting program. The result of fit is compared with experimental data in Fig. 10. It may be worth mentioning that each experimental data on Fig. 10 represents a unique case of weather condition for the day the measurement was carried out (event). Corresponding theoretical points are those estimated by Eq. (1). It is clear that there is a good agreement between the two sets of results. The values of the three fitted parameters and their corresponding 95% confidence level ranges are presented in Table 2.

It is interesting to note that these fitted values of a_1, a_2, and a_3 indicate with 95% confidence level probability that the total daily solar radiation carries the major weight in affecting the still productivity. This weight is in the range of 85%–100%. The temperature and wind effects maximum estimated contributions are 17% and 13%, respectively.

In order to check the model predictions against similar experimental works, one need data for the daily solar radiation, maximum temperature, mean wind speed, and productivity for a still of similar design. These proved difficult to find in published literature. However, some useful such data for 1 d operation of a 45° pyramid shaped still were found

Table 3
Model productivity predictions using data from reference [49]

Daily solar radiation (kWh)	Maximum day temperature (°C)	Mean wind speed (km h^{-1})	Still experimental productivity (cm^3 m^{-2}.d)	Model productivity (cm^3 m^{-2}.d) with a_1 0.997, a_2 0.003, a_3 0.003	Model productivity (cm^3 m^{-2}.d) with a_1 0.85, a_2 0.15, a_3 0.00	Model productivity (cm^3 m^{-2}.d) with a_1 0.78, a_2 0.21, a_3 0.01
2.73	24.2	35.2	602	443	450	608

in Table 1 [49]. After adjusting for still area, and integrating over total daily solar radiation, the input data for the model shown in the first column of Table 1 are substituted in the model Eq. (1). Three sets of partial contributions parameters a_1, a_2, and a_3 are selected and the daily productivity of the still is calculated for each set. The results are in the last column of Table 3.

These results suggest that there is about 25% difference between experimental and model predicted daily productivity values when parameter values derived for our solar still are used. This is not surprising because of the difference in still geometry, water depth and so on. Even so, the model succeeded in predicting a productivity of 608 cm^3 m^{-2}.d compared with the experimental value of 602 cm^3 m^{-2}.d when the contributions parameters are set to 78%, 21%, and 1% to be due to solar, temperature, and wind, respectively. This suggests that ambient temperature effects are more significant in the case of large angle pyramid shaped still cover compared with that for single lower inclination cover still.

5. Conclusions

The empirical model constructed on the basis of the assumption that the productivity of a single inclined cover solar still can be determined by three weather parameters. These are input solar energy, the maximum daylight temperature, and mean wind speed. An associated empirical relation can describe each of the three parameters effect. First stage fitting of experimental data can determine each of the three empirical functions. Second stage fitting allows for the determination of the contributing weight of each of three independent variables. The model predictions compare well with our experimental data. Fitting results suggest that the total daily solar radiation plays the most important role in the still operation. Even so, the application of the model to other independent published experimental data suggests that changing shape and inclination angle of the glass cover and water depth and so on may significantly increase temperature and to some extent wind speed effect at the expense of solar effect.

References

[1] R. Ward, Lloyd's, Global Water Scarcity Risks and Challenges for Business, 2010, Available from: http://awsassets.panda.org/downloads/lloyds_global_water_scarcity.pdf.

[2] UNESCO Publication. The United Nations World Water Development Report Water for People Water for Life, 2000, Available from: http://www.un.org/esa/sustdev/publications/WWDR_english_129556e.pdf.

[3] V. Srinivasan, E.F. Lambin, S.F. Gorelick, B.H. Thompson, S. Rozelle, The nature and causes of the global water crisis: syndromes from a meta-analysis of coupled human-water studies, Water Resour. Res., 48 (2012) 1–16.

[4] A.Y. Hoekstra, M.M. Mekonnen, Global Water Scarcity, UNESCO, 2011.

[5] United Nation Global Compact Climate Change and the Global Water Crisis: What Businesses Need to Know and Do Pacific Institute, 2009, Available from: http://ceowatermandate.org/files/research/UNGC-PI_climate-water_whitepaper_FINAL.pdf.

[6] F. Ackerman, E.A. Stanton, The Last Drop: Climate Change and the Southwest Water Crisis. Stockholm Environment Institute-U.S. Center, 2011, Available from: http://sei-us.org/Publications_PDF/SEI-WesternWater-0211.pdf.

[7] P.H. Gleick, Water, war and peace in the Middle East, Environment, 36 (1994) 7–42.

[8] H. Bigas, T. Morris, B. Sandford, Z. Adeel, The Global Water Crisis: Addressing an Urgent Security Issue, 2012, Available from: http://inweh.unu.edu/wp-content/uploads/2013/05/WaterSecurity_The-Global-Water-Crisis.pdf.

[9] A. Al-Karaghouli, D. Renne, L. Kazmerski, Solar and wind opportunities for water desalination in the Arab regions, Renew. Sustainable Energy Rev., 13 (2009) 2397–2407.

[10] WateReuse Association, Seawater Desalination Power Consumption, 2011, Available from: https://www.watereuse.org/sites/default/files/u8/Power_consumption_white_paper.pdf.

[11] M. Goosen, H. Mahmoudi, N. Ghaffour, S. Sablani, Application of Renewable Energies for Water Desalination, Desalination, Trends and Technologies, InTech, 2011, pp. 89–118.

[12] H. Cooley, M. Heberger, Key Issues for Seawater Desalination in California Energy and Greenhouse Gas Emissions Pacific Institute, 2013, www.pacinst.org/reports/desalination_2013/energy.

[13] The World Bank Publication, Renewable Energy Desalination: An Emerging Solution to Close the Water Gap in the Middle East and North Africa, 2012, Available from: http://water.worldbank.org/sites/water.worldbank.org/files/publication/water-wpp-Sun-Powered-Desal-Gateway-Meeting-MENAs-Water-Needs_2.pdf.

[14] A.F. Mashalya, A.A. Alazbaa, A.M. Al-Awaadh, Assessing the performance of solar desalination system to approach near-ZLD under hyper arid environment, Desal. Water Treat., 57 (2016) 12019–12036.

[15] E. Delyannis, A.A. El-Nashar, Renewable Energy System and Desalination – Vol. I - A Short Historical Review of Renewable Energy, Encyclopedia of Desalination and Water Resources (DESWARE), 2014, Available from: http://www.desware.net/DESWARE-SampleAllChapter.aspx.

[16] S.A. Kalogirou, Seawater desalination using renewable energy sources, Prog. Energy Combust. Sci., 31 (2005) 242–281.

[17] O. Badran, Theoretical analysis of solar distillation using active solar still, Int. J. Therm. Environ. Eng., 3 (2011) 113–120.

[18] D.W. Medugu, L.G. Ndatuwong, Theoretical analysis of water distillation using solar still, Int. J. Phys. Sci., 4 (2009) 705–12.

[19] S. Shanmugan, B. Janarathanan, J. Chandrasekaran, Thermal asymmetry model of single slope single basin solar still with sponge liner, Therm. Sci., 18 (2014) S339–S350.

[20] T. Fukuhara, A. Ahasan, Y. Ishii, Production Model of Tubular Solar Still Based on Condensation Theory, IV Conferencia Latino Americana de Energia Solar ISES_CLA)y XVII Symposio Peruana de Energia Solar (XVII-SPES), Cusco, 1–5.11.2010.
[21] E.O. Osafile, O.D. Ojuh, Estimation of the production of a solar still, Int. J. Eng. Sci., 2 (2013) 76–80.
[22] B. Gupta, T.K. Mandraha, P. Edla, M. Pandya, Thermal modeling and efficiency of solar water distillation: a review, Am. J. Eng. Res., 2 (2013) 203–213.
[23] R. Alvarado-Juárez, J. Xamán, G. Álvarez, I. Hernández-López, Numerical study of heat and mass transfer in a solar still device: effect of the glass cover, Desalination, 359 (2015) 200–211.
[24] N. Rahbar, J.A. Esfahani, Productivity estimation of a single-slope solar still: theoretical and numerical analysis, Energy, 49 (2013) 289–297.
[25] R. Alvarado-Juárez, G. Álvarez, J. Xamán, I. Hernández-López, Numerical study of conjugate heat and mass transfer in a solar still device, Desalination, 325 (2013) 84–96.
[26] A. Omri, J. Orfi, S.B. Nasrallah, Natural convection effects in solar stills, Desalination, 183 (2005) 173–178.
[27] A. Dehghan, A. Afshari, N. Rahbar, Thermal modeling and exergetic analysis of a thermoelectric assisted solar still, Sol. Energy, 2115 (2015) 277–288.
[28] N. Rahbar, A. Esfahani, E. Fotouhi-Bafghi, Estimation of convective heat transfer coefficient and water-productivity in a tubular solar still – CFD simulation and theoretical analysis, Sol. Energy, 113 (2015) 313–323.
[29] N. Rahbar, J.A. Esfahani, Estimation of convective heat transfer coefficient in a single-slope solar still: a numerical study, Desal. Water Treat., 50 (2012) 387–396.
[30] PCE Instruments UK Ltd, Hampshire, UK. Available at: http://www.industrial-needs.com/technical-data/solar-radiation-meter-pce-spm1.htm
[31] M. Kottek, J. Grieser, C. Beck, F. Rubel, World Map of the Köppen-Geiger climate classification updated, Meteorologische Zeitschrift, 15 (2006) 259–263. Available at: http://koeppen-geiger.vu-wien.ac.at/pdf/kottek_et_al_2006_A4.pdf
[32] Metablue weather archives. Available at: https://www.meteoblue.com/en/weather/forecast/archive/mosul_iraq_99072
[33] A.A. Azooz, Acquiring numerical data from an oscilloscope screen pictures, Instrum. Exp. Tech+, 54 (2011) 364–368.
[34] S. Nijmeh, S. Odeh, B. Akash, Experimental and theoretical study of a single-basin solar still in Jordan, Int. J. Heat Mass Transfer, 32 (2005) 565–572.
[35] C.N.O. Kwach, R.M. Ochieng, F.N. Onyango, Investigation of some factors that lead to improved performance vis-a-vis the efficiency of single basin solar stills, J. Fund. Renew. Energy Appl., 1 (2011) 1–6.
[36] P.R. Prasad, P. Pujitha, B.G.V. Rajeev, K. Vikky, Energy efficient solar water still, Int. J. Chem. Tech. Res., 3 (2011) 1781–1787.
[37] A. Mehta, A. Vyas, N. Bodar, D. Lathiya, Design of solar distillation system, Int. J. Sci. Adv. Technol., 29 (2011) 67–74.
[38] C. Tenthani, A. Madhlopa, C.Z. Kimambo, Improved solar still for water purification, J. Sust. Energy Environ., 3 (2012) 111–113.
[39] S.H. Sengar, Y.P. Khandetod, A.G. Mohod, New innovation of low cost solar still, Eur. J. Sustain. Dev., 1 (2012) 315–352.
[40] P. Refalo, R. Ghirlando, S. Abela, The effect of climatic parameters on the heat transfer mechanisms in a solar distillation still, Heat Transfer. Eng., 35 (2012) 1473–1481.
[41] N.S. Patel, R.R. Shah, N.M. Patel, J.K. Shah, S.B. Bhatt, Effect of various parameters on different types of solar still: case study, Int. J. Innov. Res. Sci. Eng. Technol., 2 (2013) 1726–1731.
[42] G.A. Al-hassan, S.A. Algarni, Exploring of water distillation by single solar still basins, Am. J. Climate Change, 2 (2013) 57–61.
[43] A.K. Sethi, V.K. Dwivedi, Design, fabrication, and performance evaluation of double slope active solar still under forced circulation mode, Int. J. Therm. Environ. Eng., 6 (2013) 27–34.
[44] M.K. Gnanadason, P.S. Kumar, V.H. Wilson, A.B. Kumaravel, B. Jebadason Comparison of performance analysis between single basin solar still made up of copper and GI, Int. J. Innov. Res. Sci. Eng. Technol., 2 (2013) 3175–3183.
[45] S.S. Priya, U.I. Mahadi, Effect of different absorbing materials on solar distillation under the climatic condition of Manipal, Int. J. Appl. Innov. in Eng. Manage., 2 (2013) 301–304.
[46] I.U. Haruna, M. Yerima, A.D. Pukuma, I.I. Sambo, Experimental investigation of the performance of basin type single-slope solar still, Int. J. Sci. Technol. Res., 3 (2014) 169–174.
[47] A. Aditya, M.V. Ramanan, Design and Development of a Low Cost Solar Still, NCREIRD Deemed University, Tamilnadu, India, 2014.
[48] P. Refalo, R. Ghirlando, S. Abela, The use of a solar chimney and condensers to enhance the productivity of a solar still, Desal. Water Treat., (2015) 1–16. doi: 10.1080/19443994.2015.1106096
[49] G.A. Al-hassan, S.A. Algarni, Exploring of water distillation by single solar still basin, Am. J. Crit. Care, 2 (2013) 57–61.